2-D LDPC Codes and Joint Detection and Decoding for Two-Dimensional Magnetic Recording

Chaitanya Kumar Matcha[1], Shounak Roy[1], Mohsen Bahrami[2], Bane Vasic[2], and Shayan Garani Srinivasa[1]

[1]Department of Electronics Systems Engineering, Indian Institute of Science, Bengaluru 560012, India
[2]Department of Electrical and Computer Engineering, The University of Arizona, Tucson, AZ 85721 USA

Two-dimensional magnetic recording (TDMR) is a promising technology for boosting areal densities (ADs) using sophisticated signal processing algorithms within a systems framework. The read/write channel architectures have to effectively tackle 2-D inter-symbol interference (ISI), 2-D synchronization errors, media and electronic noise sources, as well as thermal asperities resulting in burst erasures. The 1-D low-density parity check (LDPC) codes are well studied to correct large 1-D burst errors/erasures. However, such 1-D LDPC codes are not suitable for correcting 2-D burst errors/erasures due to the 2-D span of errors. In this paper, we propose construction of a native 2-D LDPC code to effectively correct 2-D burst erasures. We also propose a joint detection and decoding engine based on the generalized belief propagation algorithm to simultaneously handle 2-D ISI, as well as correct bit/burst errors for TDMR channels. This paper is novel in two aspects: 1) we propose the construction of native 2-D LDPC codes to correct large 2-D burst erasures and 2) we develop a 2-D joint signal detection-decoder engine that incorporates 2-D ISI constraints, and modulation code constrains along with LDPC decoding. The native 2-D LDPC code can correct >20% more burst erasures compared with the 1-D LDPC code over a 128 × 256 2-D page of detected bits. Also, the proposed algorithm is observed to achieve a signal-to-noise ratio gain of >0.5 dB in bit error rate performance (translating to 10% increase in ADs around the 1.8 Tb/in^2 regime with grain sizes of 9 nm) as compared with a decoupled detector-decoder system configuration over a small 2-D LDPC code of size 16 × 16. The efficacy of our proposed algorithm and system architecture is evaluated by assessing AD gains via simulations for a TDMR configuration comprising of a 2-D generalized partial response over the Voronoi media model assuming perfect 2-D synchronization.

Index Terms— **TDMR. LDPC, 2D burst erasure correction, joint detection-decoding, GBP.**

I. Introduction

TWO-DIMENSIONAL magnetic recording (TDMR) aims at improving areal densities beyond 1 Tb/in^2 by packing tracks closely, allowing for 2-D inter-symbol interference (ISI) [1]. The effects of bit-size reduction are handled using sophisticated signal processing algorithms. Along with the random errors due to channel impairments, we also observe burst erasures in magnetic recording channels due to thermal asperities, inherent defects on the recording medium, scratches on the recording surface, or due to external mechanical shocks/vibrations [2]. This requires sophisticated signal detection and strong error correcting codes (ECCs), to meet stringent [sector failure rate (SFR) ~ $1e-15$] reliability requirements.

A. Burst Erasure Correction for TDMR

Low-density parity check (LDPC) codes have been widely studied and are successfully deployed in hard disk drives due to excellent error correction abilities and amenable to silicon implementation. Systematically constructed quasi-cyclic (QC) LDPC codes [3] using permutation matrices help in efficient implementation of the LDPC decoder architectures using variants of the belief propagation (BP) algorithm. QC-LDPC codes are also observed to give good 1-D burst erasure correction capability [2]. The LDPC decoders are aided by defect detectors in the read channel for estimating the locations of erasures, which are flag to the LDPC decoder for burst erasure correction [4], [5].

Matcha and Srinivasa [6] have proposed a 2-D defect detector using 1-D QC-LDPC codes with various interleaving schemes for 2-D burst erasure correction in TDMR. The 1-D LDPC code is populated into a 2-D page in the raster scan order. The study of ECCs for 2-D burst error/erasure correction has been restricted to algebraic codes that can correct a predefined pattern of errors with guaranteed error correction ability [7], [8]. These 2-D codes are not suitable for correction of large burst errors/erasures.

The 1-D burst erasure correction capability of LDPC codes can be studied using zero spans in the parity check matrix. Fossorier [9] has proved that most LDPC codes can achieve burst erasure correction capability achieving the Roger bound, i.e., an (n, k) code correcting up to $(n-k-1)$ length of burst erasure. In this paper, we extend the idea of 1-D QC-LDPC code construction and propose a native 2-D LDPC code with good 2-D burst erasure correction capability. We also study the burst erasure correction capability of the proposed code using the zero spans in the parity check matrix.

B. Efficient Detection and Decoding Architectures

The 2-D signal detection algorithms can be broadly classified into trellis-based approaches and those derived using the generalized BP (GBP) algorithm. Examples to the trellis class of algorithms include [10]–[12] and so on. Trellis-based approaches achieve maximum-likelihood performance locally (i.e., over a multi-rows and columns). Near optimal

Manuscript received June 19, 2017; accepted July 24, 2017. Date of publication August 9, 2017; date of current version January 18, 2018. Corresponding author: S. G. Srinivasa (e-mail: shayangs@iisc.ac.in).

Color versions of one or more of the figures in this paper are available online at http://ieeexplore.ieee.org.

Digital Object Identifier 10.1109/TMAG.2017.2735181

2-D maximum *a posteriori* probability (MAP) performance can be achieved by coupling 2-D soft equalizers with iterative multi-row/column detectors within an iterative set up [10] using 2-D generalized partial response targets [11]. On the other hand, the GBP algorithm operates over an entire 2-D page using a region-based hierarchy. This algorithm is empirically observed to provide marginal estimates, close to true marginals at the expense of huge computational complexity. The state-of-the-art work on coding and detection for TDMR channels includes coupling soft detectors with 1-D iterative ECCs such as LDPC codes to realize significant signal-to-noise ratio gains [6]. It must be noted that the signal detectors and the ECC decoders are optimized separately using different criteria even though they are coupled through a turbo loop.

Intuitively, improved performance can be accomplished by fusing a signal detector with an error correction decoder using message passing equations over the joint detection-decoder engine. The message passing equations are derived from the same cost function, unlike earlier approaches. Kurkoski *et al.* [13] considered the idea of fusing the partial response channel with parity check constraints to form joint factor graphs and obtained message passing decoders that showed better performance than individually optimized detectors and decoders over the perpendicular magnetic recording channel. In this paper, we extend the notion of joint 2-D detection and decoding toward TDMR channels. It must be noted that there are several significant differences between the 1-D joint detector-decoder engine [13] and the 2-D case. First, we introduce a novel 2-D LDPC code with parity check equations represented by a 3-D tensor using a composition of tiles of permutations matrices in 2-D. This code is inherently 2-D and resilient to 2-D burst erasures and random errors. Second, we introduce the parity check constraints directly into the formulation of the Gibbs free energy. Using a constrained optimization framework, we derive the message passing equations using the same cost function from the first principles by tracking the ancestors of all bits within a region using ancestors corresponding to the ISI and the parity check constraints. We study the efficacy of our new algorithm and joint detector-decoder architecture over individual detector and decoder engines coupled via a turbo loop. This framework can be extended for fusing a broad class of signal detectors and code constraints toward a hybrid architecture.

C. Paper Organization

This paper is organized as follows. In Section II, we propose a novel 2-D LDPC code construction for correcting burst erasures in TDMR. In Section III, we formulate GBP for joint detection and decoding by considering 2-D ISI and LDPC code constraints. In Section IV, we present and discuss our simulation results using a Voronoi-based TDMR channel model. Section V concludes this paper.

II. LDPC Code for 2-D Burst Erasure Correction

LDPC codes are observed to give near Shannon-capacity performance. These codes are successfully deployed in magnetic storage as well as in other storage technologies, such as flash memories and optical storage devices, due to amenable hardware architectures for realizing the algorithms in practice.

For magnetic recording channels, the ECC should be able to correct random errors as well as burst erasures that are often seen due to thermal asperities [14]. This requires us to construct LDPC codes that can correct large burst erasures along with a mix of random errors. Fossorier [9] proved that LDPC parity check matrices can be written in burst correction form (BCF) that enables us to correct 1-D burst erasures achieving the Roger bound, i.e., an (n, k)-code that can correct erasures of length up to $n-k$. However, the BCF of the parity check matrix has a large number of parity check equations that makes it unsuitable for practical decoding using the BP algorithm. QC-LDPC codes provide a regular construction of the LDPC parity check matrix, and are observed to give a good 1-D burst erasure correction performance. Other techniques to improve burst erasure correction capability of LDPC codes include permuting the code word using simulated annealing [15], or by studying trapping sets of the code [16], [17].

For TDMR, we model the burst erasures as a random 2-D connected shape. Algebraic code construction for 2-D burst error correction is studied by Roy and Srinivasa [7] and Yoon and Moon [8]. However, these codes are designed for very small burst errors of predefined shapes. Cassuto and Shokrollahi [18] have proved existential results of 2-D LDPC codes based on the ideas of array codes. However, LDPC code construction to correct 2-D burst erasures is not explicitly provided. Matcha and Srinivasa [6] have used 1-D LDPC codes for 2-D burst erasure correction by rasterizing 1-D code words into a 2-D page along with interleavers. However, these codes are not constructed and optimized to correct large 2-D burst erasures. In this section, we extend the ideas of 1-D QC-LDPC code construction toward a native 2-D LDPC code that can effectively correct 2-D burst erasures than without it.

A. 2-D LDPC Code Construction

The 1-D QC-LDPC codes [3] are constructed using parity check matrices realized as a tiling of permutation matrices. If $\mathbf{I}$ is an identity matrix of size $p \times p$ and $\mathbf{P}$ is a permutation matrix of the same size, an example parity check matrix with row weight r and column weight c is given by

$$\mathbf{H}_{\text{1-D}} = \begin{bmatrix} \mathbf{I} & \mathbf{I} & \mathbf{I} & \cdots & \mathbf{I} \\ \mathbf{P} & \mathbf{P}^2 & \mathbf{P}^3 & \cdots & \mathbf{P}^r \\ \mathbf{P}^2 & \mathbf{P}^4 & \mathbf{P}^6 & \cdots & \mathbf{P}^{2r} \\ \vdots & \vdots & \vdots & \ddots & \vdots \\ \mathbf{P}^{c-1} & \mathbf{P}^{2c-2} & \mathbf{P}^{3c-3} & \cdots & \mathbf{P}^{r(c-1)} \end{bmatrix}. \quad (1)$$

A typical choice of the permutation matrix is a unit-circular shift matrix given by

$$\mathbf{P} = \begin{bmatrix} 0 & 1 & 0 & \cdots & 0 \\ 0 & 0 & 1 & \cdots & 0 \\ \vdots & \vdots & \vdots & \ddots & \vdots \\ 0 & 0 & 0 & \cdots & 1 \\ 1 & 0 & 0 & \cdots & 0 \end{bmatrix}. \quad (2)$$

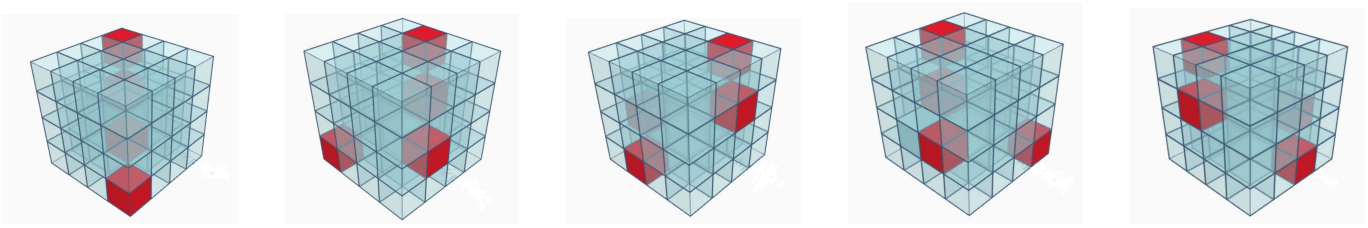

(a) (b) (c) (d) (e)

Fig. 1. Identity tensor and the row and column permutations of the tensor. (a) Identity tensor $\mathbf{I}$. (b) One row shift: $P(\mathbf{I})$. (c) Two row shifts: $P^2(\mathbf{I})$. (d) One column shift: $Q(\mathbf{I})$. (e) Two column shifts: $Q^2(\mathbf{I})$.

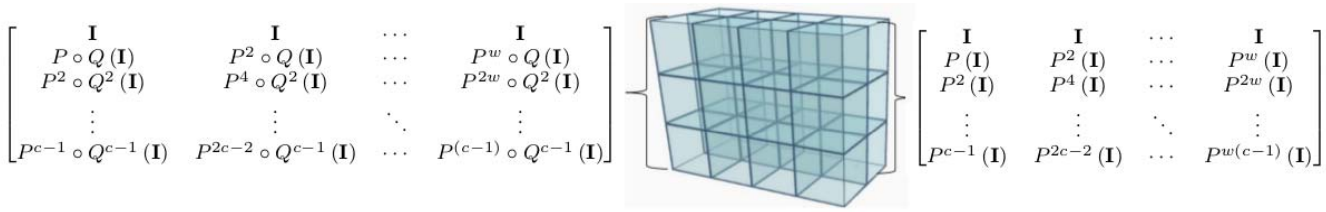

Fig. 2. Example of a parity check tensor for a 2-D LDPC code. The building blocks are the identity tensor and its row and column permutations.

The powers of $\mathbf{P}$ in the construction of $\mathbf{H}_{1\text{-D}}$ give tiles with different shifts. The choice of the permutation matrix and the shifts provide us with a variety of QC-LDPC codes.

The burst erasure correction capability of 1-D QC-LDPC can be explained using the zero span of the code: a code will be able to correct burst erasure of length l if for every position j in the code word, there exists an ith row in $\mathbf{H}_{1\text{-D}}$ such that $h_{ij} = 1$ and $h_{i(j+1)} = h_{i(j+2)} = \cdots = h_{i(j+l-1)} = 0$. The condition essentially ensures that the jth bit erasure can be corrected using ith parity check equation.

We extend these ideas to construct 2-D LDPC codes. The code word of a 2-D LDPC code is a 2-D page of bits. Therefore, the words orthogonal to the 2-D LDPC codes are also 2-D page of bits. The parity check equations will be represented by a 3-D parity check tensor obtained by stacking these orthogonal words one below the other. Each layer of the parity-check tensor represents a single parity check equation.

We propose the construction of the parity check tensor by stacking 3-D permutation tensors in a 3-D fashion. We use the indexing notation such that the position (i, j, k) represents the (j, k) bit in the ith layer of the parity check tensor. We consider an identity tensor $\mathbf{I}$ of size $p \times p \times p$ given by

$$\mathbf{I} = [I_{i,j,k}]_{i,j,k=1}^{p}, \quad I_{i,j,k} = \begin{cases} 1, & i = j = k \\ 0, & \text{otherwise.} \end{cases}$$

The tensor $\mathbf{I}$ can be permuted in two directions. Let $P : \{1, 2, \ldots, p\} \to \{1, 2, \ldots, p\}$ and $Q : \{1, 2, \ldots, p\} \to \{1, 2, \ldots, p\}$ be the permutation operations defined on any tensor $\mathbf{T} = [T_{i,j,k}]_{i,j,k=1}^{p}$ as

$$P(\mathbf{T}) = [T_{i,P(j),k}]_{i,j,k=1}^{p} \text{ and } Q(\mathbf{T}) = [T_{i,j,Q(k)}]_{i,j,k=1}^{p}.$$

Proposition 1 proves the properties of row and column permutations described in this section.

Proposition 1: If $P(\mathbf{T}) = [T_{i,P(j),k}]_{i,j,k=1}^{p}$ and $Q(\mathbf{T}) = [T_{i,j,Q(k)}]_{i,j,k=1}^{p}$ are row and column permutations operating on a tensor, the following properties hold true.

1) $P \circ Q(\mathbf{T}) = Q \circ P(\mathbf{T})$.
2) In general, any order of m permutations of P and n permutations of Q on $\mathbf{T}$ can be written as $P^m \circ Q^n(\mathbf{T})$.

Proof: From the definitions of P and Q, we have

$$P \circ Q(\mathbf{T}) = P\left([T_{i,j,Q(k)}]_{i,j,k=1}^{p}\right) = [T_{i,P(j),Q(k)}]_{i,j,k=1}^{p}.$$

Similarly

$$Q \circ P(\mathbf{T}) = Q\left([T_{i,P(j),k}]_{i,j,k=1}^{p}\right) = [T_{i,P(j),Q(k)}]_{i,j,k=1}^{p}.$$

This proves the first property that the order of row and column permutations can be interchanged. The second property follows from the first by exchanging adjacent P and Q in such a way that all Ps appear on the left and all Qs appear on the right. ■

Since P and Q are permutations of p elements, we have $P^p(\boldsymbol{T}) = \boldsymbol{T}$; $Q^p(\boldsymbol{T}) = \boldsymbol{T}$ and $P^{np+r}(\boldsymbol{T}) = P^r(\boldsymbol{T})$; $Q^{np+r}(\boldsymbol{T}) = Q^r(\boldsymbol{T})$, where n is any integer and $0 \le r < p$.

Similar to the 1-D QC-LDPC code construction, we can construct the 2-D LDPC tensor $\mathbf{H}_{2\text{-D}}$ using various permutations of the identity tensor $\mathbf{I}$ using the permutations P and Q. Each permutation of $\mathbf{I}$ gives us a cube. A $\mathbf{H}_{2\text{-D}}$ can be obtained by stacking $c \times h \times w$ cubes along (i, j, k) directions, respectively.

Similar to the permutation in (2), we choose the permutations P and Q to be circular shifts given by

$$P(i) = Q(i) = \begin{cases} 1, & i = p \\ i + 1, & \text{otherwise.} \end{cases}$$

The identity tensor along with its row column permutations is shown in Fig. 1.

We can also construct $\mathbf{H}_{2\text{-D}}$ similar to $\mathbf{H}_{1\text{-D}}$ in (1), where the (x, y, z)th cube in the stack is given by $P^{x(z-1)} \circ Q^{x(y-1)}(\mathbf{I})$.

Fig. 2 shows the pictorial representation of an example $\mathbf{H}_{2\text{-D}}$ constructed using the above-mentioned idea.

B. Design of 2-D LDPC Code for TDMR

The shifts/powers of the permutations used in the construction of $\mathbf{H}_{2\text{-D}}$ for our purpose are chosen as follows. The $\mathbf{H}_{2\text{-D}}$ is constructed by stacking $c \times h \times w$ cubes, each of size $p \times p \times p$ such that c is a multiple of p.

In our code construction, the (i, j, k)th cube is given by $P^{a(i,j,k)} \circ Q^{b(i,j,k)}(i)$, where the powers $a(i, j, k)$ and $b(i, j, k)$ are chosen as

$$a(i, j, k) = i \mod p \tag{3}$$

$$b(i, j, k) = \left\lfloor \frac{i-1}{p} \right\rfloor jk. \tag{4}$$

Notice that each cube in $\mathbf{H}_{2\text{-D}}$ contributes only to p bits for the column weight. Therefore, it is important to choose the shifts such that every bit position in the code word has sufficient column weight for good error correction. Lemma 1 shows that the above-mentioned choice of shifts give a uniform column weight of (c/p).

Lemma 1: Stacking $c \times h \times w$ cubes with the shifts given in (3) and (4) gives a parity check tensor with uniform column weight of (c/p).

Proof: We prove this by showing that the column weight contributed by the stack of cubes $\{(i, j, k) \mid (p-1)n < i \leq np\}$ is uniformly 1 at all code-word positions within the stack for all $(j, k) \in \{1, 2, \cdots p\}^2$ and $n = 1, 2, \ldots, (c/p)$.

The set of positions contributing to column weight by identity cube is given by

$$P^{(1,1,1)} = \{(x, x) \mid 1 \leq x \leq p\}.$$

The set of positions contributing to column weight by (i, j, k)th cube is given by

$$P^{(i,j,k)} = \left\{ \left(P^{i \mod p}(x), Q^{\left\lfloor \frac{i-1}{p} \right\rfloor jk}(x) \right) \mid 1 \leq x \leq p \right\}.$$

The set of positions contributing to column weight by the stack $\{(i, j, k) \mid (p-1)n < i \leq np\}$ cube is given by

$$P_n^{(j,k)} = \bigcup_{i=(p-1)n+1}^{np} \left\{ \left(P^{i \mod p}(x), P^{\left\lfloor \frac{i-1}{p} \right\rfloor jk}(x) \right) \right. \tag{5}$$

$$\left. \mid 1 \leq x \leq p \right\} \tag{6}$$

$$= \bigcup_{i'=1}^{p} \{(P^{i'}(x), Q^{njk}(x)) \mid 1 \leq x \leq p\} \tag{7}$$

$$= \left\{ (P^{i'}(x), Q^{njk}(x)) \mid 1 \leq x \leq p, \right. \tag{8}$$

$$\left. 1 \leq i' \leq p \right\} \tag{9}$$

$$= \bigcup_{x=1}^{p} \{(P^{i'}(x), Q^{njk}(x)) \mid 1 \leq i' \leq p\} \tag{10}$$

$$= \bigcup_{x=1}^{p} \{(i', Q^{njk}(x)) \mid 1 \leq i' \leq p\} \tag{11}$$

$$= \bigcup_{x=1}^{p} \{(i', x) \mid 1 \leq i' \leq p\} \tag{12}$$

$$= \{(i', x) \mid 1 \leq i' \leq p,\ 1 \leq x \leq p\}. \tag{13}$$

Step (11) uses the fact that the row permutations are complete, that is

$$\{P^i(x) \mid 1 \leq i \leq p\} = \{1, 2, \cdots p\} \quad \forall 1 \leq x \leq p.$$

Step (12) uses the fact that the column permutation is a one-to-one mapping, that is

$$\{Q^i(x) \mid 1 \leq x \leq p\} = \{1, 2, \cdots p\} \quad \forall 1 \leq i \leq p.$$

Therefore, we have proven that each $p-$stack at position (j, k) given by $\{(i, j, k) \mid (p-1)n < i \leq np\}$ contributes to a column weight of 1 at every corresponding code-word position. Since there are (c/p) such $p-$stacks, the constructed code has a uniform column weight of (c/p). ■

Remarks:

1) Each cube contributes to a row weight of exactly 1. Therefore, the row weight of the code constructed by stacking $c \times h \times w$ cubes is hw.
2) If c is not a multiple of p, the column weights can be bounded as $\lfloor (c/p) \rfloor \leq r \leq \lceil (c/p) \rceil$.

C. Burst Erasure Correction Capability of the 2-D LDPC Code

Similar to the 1-D QC-LDPC code, we analyze the burst error correction capability of the code using the zero spans on the parity check tensor $\mathbf{H}_{2\text{-D}}$ using Lemma 2.

Lemma 2: A 2-D ECC with parity check tensor $\mathbf{H}_{2\text{-D}} = [h_{i,j,k}]$ can correct up to a 2-D burst of size $B_h \times B_w$ if for every position (j, k), there exists ith layer in $\mathbf{H}_{2\text{-D}}$ such that

$$h_{i,a,b} := \begin{cases} 1, & (a, b) = (j, k) \\ 0, & (a, b) \in \{(j + x, k + y) \mid -B_h \\ & < x < B_h, |-B_w < y < B_w\} \setminus \{(j, k)\}. \end{cases} \tag{14}$$

Proof: The condition in (14) means that the ith parity check equation uses only the (j, k)th bit within the erasure region.

Let the $B_h \times B_w$ burst erasure occur with the starting position of (s_h, s_w), i.e., the erasure locations are given by

$$R = \{(s_h + x, s_w + y) \mid 0 \leq x < B_h, 0 \leq y < B_w\}.$$

We prove the result by showing that each bit in the burst erasure can be corrected independently using the condition given in (14). For the position (s_h, s_w), the condition in (14) ensures that there is a parity check equation such that the bits in

$$R_{(s_h,s_w)} = \{(s_h + x, s_w + y) \mid -B_h \leq x < B_h, \\ -B_w \leq y < B_w\} \setminus \{(s_h, s_w)\}$$

are not involved. Since $R \setminus \{(s_h, s_w)\} \subset R_{(s_h,s_w)}$, none of the bits in the erasure location except for the (s_h, s_w)th bit is used in this parity check equation. This allows us to correct the (s_h, s_w)th bit using this parity check equation.

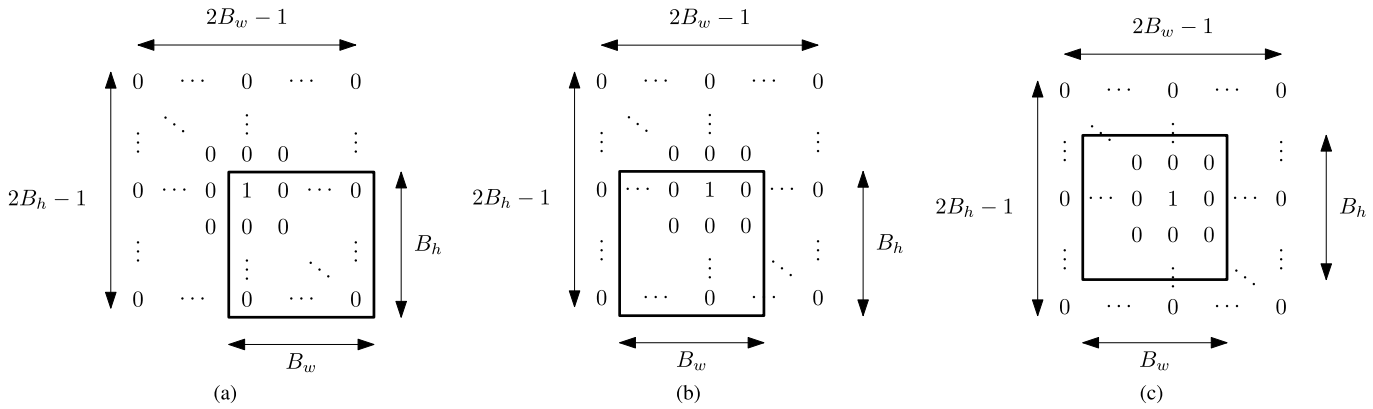

Fig. 3. Span of $(2B_h - 1) \times (2B_w - 1)$ zeros around a 1 in each parity check layer can help in correcting a burst of size at least $B_h \times B_w$. The burst erasure region is indicated using a rectangle relative to various locations within erasure region. This condition ensures that every location within the burst erasure can be corrected using the parity check equation, since the remaining bits are not involved in the corresponding parity check equation. (a) Correcting the starting position of the burst erasure. (b) Correcting a bit in the first row of the burst erasure. (c) Correcting an arbitrary bit within the burst erasure.

Similarly, for any location $(s_h + j, s_w + k)$, $0 \le j < B_h$, $0 \le k < B_w$, the condition in (14) ensures that there is a parity check equation such that the bits in

$$\begin{aligned} &R_{(s_h+j,s_w+k)} \\ &\quad = \{(s_h + j + x, s_w + k + y) \mid -B_h \le x < B_h \\ &\qquad\qquad -B_w \le y < B_w\} \setminus \{(s_h + j, s_w + k)\} \\ &\quad = \{(s_h + x, s_w + y) \mid -B_h + j \le x < B_h + j \\ &\qquad\qquad -B_w + k \le y < B_w + k\} \setminus \{(s_h + j, s_w + k)\} \end{aligned}$$

are not involved. For $0 \le j < B_h$, $0 \le k < B_w$, it is easy to verify that $R \subset R_{(s_h+j,s_w+k)} \setminus \{(s_h + j, s_w + k)\}$. Therefore, the parity check equation can be used to correct the bit at location $(s_h + j, s_w + k)$. This is shown in Fig. 3(c).

This proves that every bit in the erasure location can be independently corrected. ∎

Theorem 1: The 2-D LDPC code constructed using the shifts in (3) and (4) can correct a 2-D burst erasure of size at least $p \times p$.

Proof: The first layer of cubes in the constructed $\mathbf{H}_{\text{2-D}}$ is a stack of identity tensors of size $p \times p \times p$. Therefore, the position of ones in the first parity check layer is given by

$$\{((j-1)p + 1, (k-1)p + 1) \mid 1 \le j \le h,\ 1 \le k \le w\}.$$

Similarly, the position of ones in the ith parity check layer is given by

$$\{((j-1)p + i, (k-1)p + i) \mid 1 \le j \le h,\ 1 \le k \le w\}.$$

Therefore, the relative positions of ones in the first p layers of $\mathbf{H}_{\text{2-D}}$ is the same as the first layer.

From (3) and (4), we have the next p layers $(p + 1 \le i \le 2p)$ obtained by a single row-shift of the top p layers. Similarly, layers from $p+1 \le i \le p^2$ are all obtained by row shifts of the first p layers. Therefore, the relative positions of ones in each of these layers $1 \le i \le p^2$ remain the same.

We can easily see that if a one is located at (j, k) in the first layer, then the following locations contain all zeros:

$$\{(j + a, k + b) \mid -p \le j \le p, -p \le k \le p\} \setminus \{(j, k)\}.$$

This is the same as the condition (14) in Lemma 2 with $B_h = p$ and $B_w = p$.

Since the relative positions of ones remain the same for the first p^2 layers, the condition (14) is satisfied for every position, where a one is present in the first p^2 layers. From Lemma 1, we have that the column weight contributed by the first p^2 layers is uniformly 1 at all positions. Therefore, the condition (14) is satisfied by every position (j, k).

Therefore, using Lemma 2, the code constructed in Section II-B can correct burst erasure of at least $p \times p$ in size. ∎

III. Joint Detection and Decoding Using GBP

GBP algorithm [19] is a graph-based decoding/detection algorithm that passes messages between regions instead of messages between nodes as in the traditional BP algorithm. GBP can be formulated as a convex optimization problem that minimizes the Gibbs free energy, and provides a method to approximate marginal distributions, which makes it suitable for MAP detection with soft outputs.

The GBP algorithm is known to give exact marginals if and only if the region-based graph has no loops [19]. When used for 2-D ISI signal detection, the region-based graphs always contain loops. However, the GBP algorithm provides a method to approximate the marginals that are empirically observed to be close to the actual marginals [20].

In order to achieve high fidelity rates (SFR $\sim 1e-15$) in magnetic recording, the detection engine is followed by an ECC decoder for error correction. The detector and the decoder often operate in a turbo loop to achieve significant gains in the performance. The BP algorithm that is used for LDPC decoding is shown to be a special case of the GBP algorithm [19]. Since the GBP-based 2-D ISI detector and the BP decoder are separately optimized, the overall performance is not guaranteed to be the best and depends on the number of turbo iterations.

In this section, we reformulate the GBP algorithm by incorporating the ECC parity-check constraints in addition to the ISI constraints toward joint detection and decoding

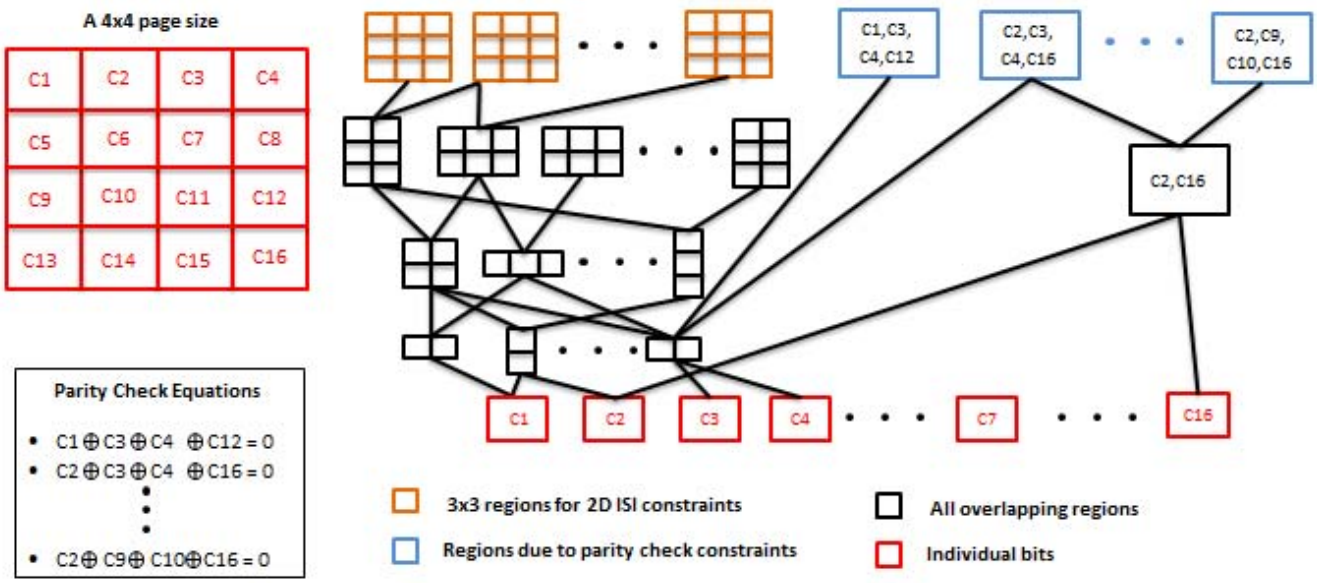

Fig. 4. Example of a region graph used by the GBP algorithm for joint detection and decoding is shown. The regions are chosen based on 2-D ISI as well as LDPC code parity check constraints.

of the readback samples. We achieve an improvement in the overall performance by incorporating ISI and LDPC constraints into a single instance of the algorithm instead of handling the constraints in two separate instances of the same GBP algorithm.

Let $x_{i,j} \in \{0, 1\}, (i, j) \in \mathbb{Z}^2$ represent bits written onto the medium after bipolar mapping and $\mathbf{x} = [x_{i,j}] \in \{0, 1\}^{n\times m}$ represent an $n \times m$ page of bits. Let $y_{i,j} \in \mathbb{R}, (i, j) \in \mathbb{Z}^2$ represent the readback samples obtained from the channel model and $\mathbf{y} = [x_{i,j}] \in \mathbb{R}^{n\times m}$ represent the corresponding page of readback samples. Let $\mathbf{x}_{i,j}$ represent the set of bits that contribute to the readback sample $y_{i,j}$. For a channel with 3×3 ISI span, $\mathbf{x}_{i,j}$ contains 9-b $\{x_{i+k,j+l} \mid k, l \in \{-1, 0, 1\}\}$. Let $\mathbf{x}_k$ represent the set of bits that are involved in the kth parity check constraint of the LDPC code for $k = 1, 2, \ldots, n_p$.

A. Gibbs Free Energy

Assuming uniform distribution of the input bits and additive white Gaussian noise in the channel model, the *a posteriori* probability of $\mathbf{x}$ given readback samples $\mathbf{y}$ is given by

$$p(\mathbf{x} \mid \mathbf{y}) = p(\mathbf{y} \mid \mathbf{x})p(\mathbf{x})p(\mathbf{y})^{-1} \propto p(\mathbf{y} \mid \mathbf{x})$$
$$p(\mathbf{y} \mid \mathbf{x}) = \prod_{i,j} f_{i,j}(\mathbf{x}_{i,j}) \tag{15}$$

where $f_{i,j}(\mathbf{x}_{i,j}) = p(y_{i,j} \mid \mathbf{x}_{i,j})$ is a Gaussian function representing the distribution of noise sample at location (i, j). Therefore, we have

$$p(\mathbf{x} \mid \mathbf{y}) = \frac{1}{Z} \prod_{i,j} f_{i,j}(\mathbf{x}_{i,j}) \tag{16}$$

for some $Z(\mathbf{y})$. Let $b(\mathbf{x})$ represent the belief of the *a posterior* probability of $\mathbf{x}$. Using the properties of KL-divergence, the belief $b(\mathbf{x}) = p(\mathbf{x} \mid \mathbf{y})$ can be achieved by minimizing the free energy given by

$$F = E - H = \mathcal{D}(b(\mathbf{x}) \parallel p(\mathbf{x} \mid \mathbf{y})) - \ln Z(\mathbf{y}) \tag{17}$$
$$\text{average energy } E = -\sum_{i,j} \sum_{\mathbf{x}_{i,j}} b(\mathbf{x}_{i,j}) \ln f_{i,j}(\mathbf{x}_{i,j}) \tag{18}$$
$$\text{entropy } H = \sum_{\mathbf{x}} b(\mathbf{x}) \ln b(\mathbf{x}). \tag{19}$$

Let a region $r \subset \mathbb{R}^2$ be defined as a set of positions within a page and $\mathcal{R}$ represent a collection of such regions.

For each $r \in \mathcal{R}$, let $\mathbf{x}_r$ be the vector of bits in the region r. Let $b(\mathbf{x}_r)$ and $p(\mathbf{x}_r)$ be the corresponding marginal beliefs and probabilities within the region r. The regions graph can be formed by partial ordering of regions based on the containment of one region inside another [19]. Fig. 4 shows an example region graph containing regions corresponding to 2-D ISI constraints as well as the LDPC constraints.

The free energy is approximated using the entropy of individual regions as

$$\hat{F} = -\sum_{i,j} \sum_{\mathbf{x}_{i,j}} b(\mathbf{x}_{i,j}) \ln f_{i,j}(\mathbf{x}_{i,j}) + \sum_{r\in\mathcal{R}} c_r \sum_{\mathbf{x}_r} b(\mathbf{x}_r) \ln b(\mathbf{x}_r) \tag{20}$$

where c_R are overcounting numbers given by

$$c_r = \sum_{p\in\mathcal{P}_r} 1 - c_p \tag{21}$$

and $\mathcal{P}_r$ are parents of region r in the region graph. This is called Kikuchi approximation, or region-based approximation.

B. Joint Detection and Decoding

When GBP is used for 2-D ISI detection as in [21], the Gibbs free energy in (20) is minimized under the

edge-constraints given by

$$\sum_{u \in \mathbf{x}_{p \setminus r}} b(\mathbf{x}_p) = b(\mathbf{x}_r) \quad \forall p \in \mathcal{P}_r \ \forall r \in \mathcal{R} \tag{22}$$

and the normalization constraints given by

$$\sum_{\mathbf{x}_r} b(\mathbf{x}_r) = 1 \quad \forall r \in \mathcal{R}. \tag{23}$$

These constraints ensure that the belief of a sub-region can be obtained by marginalizing the beliefs of their parents [19]. The GBP algorithm is obtained from the constrained optimization of $\hat{F}$ using Lagrange multipliers.

The choice of regions and c_r influence the behavior of the algorithm as follows.

1) Choice of c_r in (21) ensures strict convexity of the free energy [22].
2) Choosing larger regions will give better approximation of the free energy.
3) Larger regions increase the computational complexity.
4) More number of regions increase the computational complexity.

In this paper, we choose the set of regions $\mathcal{R}$ such that it has the following.

1) Regions $\mathbf{x}_{i,j}$, corresponding to each 2-D ISI constraint, are included.
2) Regions $\mathbf{x}_k$, corresponding to each parity check constraint, are included.
3) Every possible intersection between the above-mentioned sets or regions is included.

For the joint detection and decoding using GBP, we ensure that the parity checks are satisfied using the LDPC constraints given by

$$b(\mathbf{x}_k) = 0, \quad \text{if parity}(\mathbf{x}_k) = 1, \ k = 1, 2, \ldots, n_p. \tag{24}$$

C. Derivation of the Joint Detection and Decoding Algorithm

In order to minimize the free energy in (20) under the constraints in (22)–(24), we define the hierarchy of regions as follows.

1) $\mathcal{A}_r$: Ancestors of the region r

$$\mathcal{A}_R = \{r' \in \mathcal{R} \mid r \subset r'\}.$$

2) $\mathcal{D}_r$: Descendants of the region r

$$\mathcal{D}_R = \{r' \in \mathcal{R} \mid r \supset r'\}.$$

3) $\mathcal{P}_r$: Parents of the region r

$$\mathcal{P}_r = \{r' \in \mathcal{R} \mid r \subset r', \nexists r'' \in \mathcal{R}, \quad r \subset r'' \subset r'\}.$$

4) $\mathcal{C}_r$: Children of the region r

$$\mathcal{C}_r = \{r' \in \mathcal{R} \mid r \supset r', \nexists r'' \in \mathcal{R}, \quad r \supset r'' \supset r'\}.$$

5) $\mathcal{A}^{(\text{ISI})}$: All ancestors of $\mathcal{R}$ arising out of ISI constraints

$$\mathcal{A}^{(\text{ISI})} = \bigcup_{(i,j)} \{\mathbf{x}_{i,j}\}.$$

6) $\mathcal{A}^{(\text{LDPC})}$: All ancestors of $\mathcal{R}$ arising out of LDPC constraints

$$\mathcal{A}^{(\text{LDPC})} = \bigcup_{p} \{\mathbf{x}_p\}.$$

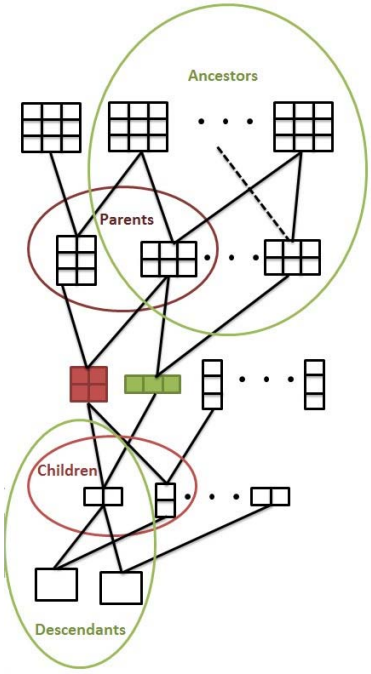

Fig. 5. Example of a region graph is shown with the relations between different regions in terms of their hierarchy. Ancestors of a region r are the set of regions that contain r. Descendants of a region r are the set of regions that are contained in r. Children of a region r are its immediate descendants. Parents of a region r are its immediate ancestors. Ancestors and descendants of the region marked in green are shown. Parents and children for the region marked in red are also shown.

7) $\mathcal{A}$: All ancestors of $\mathcal{R}$

$$\mathcal{A} = \mathcal{A}^{(\text{ISI})} \cup \mathcal{A}^{(\text{LDPC})} = \{r \in \mathcal{R} \mid \nexists r' \in \mathcal{R}, \quad r' \supset r\}.$$

Fig. 5 shows an example region graph illustrating the relations between different regions in terms of their hierarchy.

We assume that none of the regions defined by LDPC constraints and ISI constraints are inclusive of each other. This implies that the bits involved in a 2-D ISI constraint are not all included in the same parity check equation. Similarly, all bits involved in a parity check equation are fully contained within the 2-D ISI span. LDPC code constructions usually satisfy this assumption and are useful for a good burst erasure correction.

Enforcing the parity constraints, we rewrite the free energy in (20) using the above-mentioned definitions as

$$\begin{aligned}\hat{F} = &- \sum_{r \in \mathcal{A}^{(ISI)}} c_r \sum_{\mathbf{x}_r} b(\mathbf{x}_r) \ln f_r(\mathbf{x}_r) \\ &+ \sum_{r \in \mathcal{R} \setminus \mathcal{A}^{(\text{LDPC})}} c_r \sum_{\mathbf{x}_r} b(\mathbf{x}_r) \ln b(\mathbf{x}_r) \\ &+ \sum_{r \in \mathcal{A}^{(\text{LDPC})}} c_r \sum_{\mathbf{x}_r : \text{parity}(\mathbf{x}_r)=0} b(\mathbf{x}_r) \ln b\ (\mathbf{x}_r).\end{aligned} \tag{25}$$

The edge constraints between a region r and its parent p in (22) can be equivalently written [19] as

$$c_r b_r(\mathbf{x}_r) + \sum_{a \in \mathcal{A}_r \setminus (\{p\} \cup \mathcal{A}_p)} c_a \sum_{\mathbf{x}_{a \setminus r}} b_a(\mathbf{x}_a) = 0. \tag{26}$$

We solve the constrained minimization of free energy [19] using Lagrange multipliers $\lambda_{pr}(\mathbf{x}_r)$, and γ_r by defining the

cost function as

$$\begin{aligned} C = &- \sum_{r\in\mathcal{A}^{(ISI)}} c_r \sum_{\mathbf{x}_r} b(\mathbf{x}_r)\ln f_r(\mathbf{x}_r) \\ &+ \sum_{r\in\mathcal{R}\setminus\mathcal{A}^{(\mathrm{LDPC})}} c_r \sum_{\mathbf{x}_r} b(\mathbf{x}_r)\ln b(\mathbf{x}_r) \\ &+ \sum_{r\in\mathcal{A}^{(\mathrm{LDPC})}} c_r \sum_{\mathbf{x}_r:\mathrm{parity}(\mathbf{x}_r)=0} b(\mathbf{x}_r)\ln b(\mathbf{x}_r) \\ &- \sum_{r\in\mathcal{R}}\sum_{p\in\mathcal{P}_r}\sum_{\mathbf{x}_r}\lambda_{pr}(\mathbf{x}_r)\times \\ &+ \left(c_r b_r(\mathbf{x}_r) + \sum_{a\in\mathcal{A}_r\setminus(\{p\}\cup\mathcal{A}_p)} c_a \sum_{\mathbf{x}_{a\setminus r}} b_a(\mathbf{x}_a)\right) \\ &- \sum_{r\in\mathcal{R}\setminus\mathcal{A}^{(\mathrm{LDPC})}} c_r\gamma_r\left(\sum_{\mathbf{x}_r} b(\mathbf{x}_r) - 1\right) \\ &- \sum_{r\in\mathcal{A}^{(\mathrm{LDPC})}} c_r\gamma_r\left(\sum_{\mathbf{x}_r:\mathrm{parity}(\mathbf{x}_r)=0} b(\mathbf{x}_r) - 1\right). \end{aligned} \tag{27}$$

We have incorporated the parity check constraints in (24) by restricting the summation of $\mathbf{x}_r$ to the words satisfying $\mathrm{parity}(\mathbf{x}_r)=1$, $\forall x \in \mathcal{A}^{(\mathrm{LDPC})}$.

For $r \in \mathcal{R}\setminus\mathcal{A}^{(\mathrm{LDPC})}$, we get

$$\begin{aligned} \frac{\partial C}{\partial b(\mathbf{x}_r)} = &-c_r\sum_{a\in\mathcal{A}_r}\ln f_a(\mathbf{x}_a) + c_r\ln b(\mathbf{x}_r) \\ &- c_r\sum_{p\in\mathcal{P}_r}\lambda_{pr}(\mathbf{x}_r) - c_r\sum_{d\in\mathcal{D}_r}\sum_{p'\in\mathcal{P}_d\setminus\{r\}}\lambda_{p'd}(\mathbf{x}_d) \\ &- c_r\gamma_r. \end{aligned} \tag{28}$$

Setting $(\partial C/\partial b(\mathbf{x}_r)) = 0$, we have

$$\begin{aligned} \ln b(\mathbf{x}_r) = &\sum_{a\in\mathcal{A}_r}\ln f_a(\mathbf{x}_a) + \sum_{p\in\mathcal{P}_r}\lambda_{pr}(\mathbf{x}_r) \\ &+ c_r\sum_{d\in\mathcal{D}_r}\sum_{p'\in\mathcal{P}_d\setminus\{r\}}\lambda_{p'd}(\mathbf{x}_d) + \gamma_r. \end{aligned} \tag{29}$$

Defining $m_{pr}(\mathbf{x}_r) = \exp(\lambda_{pr}(\mathbf{x}_r))$, we have

$$\begin{aligned} b(\mathbf{x}_r) = &\exp(\gamma_r)\prod_{a\in\mathcal{A}_r} f_a(\mathbf{x}_a)\prod_{p\in\mathcal{P}_r} m_{pr}(\mathbf{x}_r) \\ &\times\prod_{d\in\mathcal{D}_r}\prod_{p'\in\mathcal{P}_d\setminus\{r\}} m_{p'd}(\mathbf{x}_d) \end{aligned} \tag{30}$$

$$\implies b(\mathbf{x}_r) \propto \prod_{a\in\mathcal{A}_r} f_a(\mathbf{x}_a)\prod_{p\in\mathcal{P}_r} m_{pr}(\mathbf{x}_r) \tag{31}$$

$$\times\prod_{d\in\mathcal{D}_r}\prod_{p'\in\mathcal{P}_d\setminus\{r\}} m_{p'd}(\mathbf{x}_d). \tag{32}$$

For $r \in \mathcal{A}^{(\mathrm{LDPC})}$ and $\mathbf{x}_r : \mathrm{parity}(\mathbf{x}_r) = 1$, we get

$$\begin{aligned} \frac{\partial C}{\partial b(\mathbf{x}_r)} = &\, c_r\ln b(\mathbf{x}_r) - c_r\sum_{p\in\mathcal{P}_r}\lambda_{pr}(\mathbf{x}_r) \\ &- c_r\sum_{d\in\mathcal{D}_r}\sum_{p'\in\mathcal{P}_d\setminus\{r\}}\lambda_{p'd}(\mathbf{x}_d) - c_r\gamma_r. \end{aligned} \tag{33}$$

Using $m_{pr}(\mathbf{x}_r) = \exp(\lambda_{pr}(\mathbf{x}_r))$, we have

$$\begin{aligned} b(\mathbf{x}_r) = &\exp(\gamma_r)\prod_{p\in\mathcal{P}_r} m_{pr}(\mathbf{x}_r) \\ &\times\prod_{d\in\mathcal{D}_r}\prod_{p'\in\mathcal{P}_d\setminus\{r\}} m_{p'd}(\mathbf{x}_d) \end{aligned} \tag{34}$$

$$\implies b(\mathbf{x}_r) \propto \prod_{p\in\mathcal{P}_r} m_{pr}(\mathbf{x}_r)\prod_{d\in\mathcal{D}_r}\prod_{p'\in\mathcal{P}_d\setminus\{r\}} m_{p'd}(\mathbf{x}_d). \tag{35}$$

Since $\mathcal{A}_r = \{\}$ for $r \in \mathcal{A}^{(\mathrm{LDPC})}$, (35) is the same as (31).

Equation (31) gives us the belief-update rules and the proportionality constant can be obtained by the normalization constraints in (23). The message update rules can be obtained using

$$\begin{aligned} \sum_{\mathbf{x}_{p\setminus r}} b(\mathbf{x}_p) = b(\mathbf{x}_r) \quad &\forall r \in \mathcal{R}\setminus\mathcal{A} \quad \forall p \in \mathcal{P}_r \\ = &\prod_{a\in\mathcal{A}_r} f_a(\mathbf{x}_a)\prod_{p''\in\mathcal{P}_r} m_{p''r}(\mathbf{x}_r) \\ &\times\prod_{d\in\mathcal{D}_r}\prod_{p'\in\mathcal{P}_d\setminus\{r\}} m_{p'd}(\mathbf{x}_d). \end{aligned} \tag{36}$$

Writing

$$\prod_{p''\in\mathcal{P}_r} m_{p''r}(\mathbf{x}_r) = m_{pr}(\mathbf{x}_r)\prod_{p''\in\mathcal{P}_r\setminus\{p\}} m_{p''r}(\mathbf{x}_r) \tag{37}$$

we can obtain $m_{pr}(\mathbf{x}_r)$ as in (38)

$$m_{pr}(\mathbf{x}_r) = \frac{\sum_{\mathbf{x}_{p\setminus r}} b(\mathbf{x}_p)}{\prod_{a\in\mathcal{A}_r} f_a(\mathbf{x}_a)\prod_{p''\in\mathcal{P}_r} m_{p''r}(\mathbf{x}_r)\prod_{d\in\mathcal{D}_r}\prod_{p'\in\mathcal{P}_d\setminus\{r\}} m_{p'd}(\mathbf{x}_d)}. \tag{38}$$

Equations (31) and (38) provide the update rules for the joint detection and decoding algorithm. Algorithm 1 summarized the joint detection and decoding engine derived in this section.

D. Remarks

It must be noted that in the formulation of the joint algorithm, the following hold.

1) Regions corresponding to LDPC constraints are considered along with the 2-D ISI constraints.
2) The beliefs of the regions corresponding to LDPC constraints are restricted to the words that satisfy the parity checks.

The implementation differs in using more regions, but ignoring the belief update equations in (31) for the words that do not satisfy parity check constraints. Similarly, if a modulation code is used for constraining 3×3 patterns, the algorithm is updated to ignore the belief update equations for the corresponding forbidden patterns.

The GBP algorithm for 2-D ISI constraints is known to be computationally very hard and is not suitable for large page sizes. In the current formulation of the GBP algorithm for joint detection and decoding, the size of the regions corresponding to LDPC constraints is dictated by the row weight of the LDPC code. Since the number of beliefs for each region depends on its size, it is practically not feasible to use this formulation of

Algorithm 1 GBP-Based Joint Detection and Decoding Algorithm

Inputs: The input page size $H \times W$, the ISI span, LDPC code parity check matrix. Region graph formed based on the ISI and LDPC constraints. $\mathcal{R}$ set of regions. $\mathcal{A}^{(\mathrm{LDPC})}$ set of regions corresponding to LDPC constraints.

Initialization: Initialize all parent to child messages m_{pc} to 1 and all beliefs to uniform distribution. Set the beliefs $b(\mathbf{x}_r) = 0$ for $r \in \mathcal{A}^{(\mathrm{LDPC})}$ when parity$(\mathbf{x}_f)$. Set iteration count $iter = 1$.

Processing:

Loop until $iter = threshold$

- **Message updates:** For each $r \in \mathcal{R}$, update messages as

$$m_{pr}(\mathbf{x}_r) = \frac{\sum_{\mathbf{x}_{p\setminus r}} b(\mathbf{x}_p)}{\prod_{a\in\mathcal{A}_r} f_a(\mathbf{x}_a) \prod_{p''\in\mathcal{P}_r} m_{p''r}(\mathbf{x}_r) \prod_{d\in\mathcal{D}_r} \prod_{p'\in\mathcal{P}_d\setminus\{r\}} m_{p'd}(\mathbf{x}_d)}$$

- **Belief updates:**
  - For each $r \in \mathcal{R} \setminus \mathcal{A}^{(\mathrm{LDPC})}$, update all beliefs

$$b(\mathbf{x}_r) = \prod_{a\in\mathcal{A}_r} f_a(\mathbf{x}_a) \prod_{p\in\mathcal{P}_r} m_{pr}(\mathbf{x}_r) \prod_{d\in\mathcal{D}_r} \prod_{p'\in\mathcal{P}_d\setminus\{r\}} m_{p'd}(\mathbf{x}_d).$$

  - For each $r \in \mathcal{A}^{(\mathrm{LDPC})}$, update beliefs only if parity$(\mathbf{x}_r) = 0$

$$b(\mathbf{x}_r) = \prod_{p\in\mathcal{P}_r} m_{pr}(\mathbf{x}_r) \prod_{d\in\mathcal{D}_r} \prod_{p'\in\mathcal{P}_d\setminus\{r\}} m_{p'd}(\mathbf{x}_d).$$

  - Normalize the beliefs to satisfy

$$\sum_{\mathbf{x}_r} b(\mathbf{x}_r) = 1$$

- Set

$$iter = iter + 1.$$

Outputs: The beliefs of 1×1 regions $b(x_{i,j})$.

the algorithm with very large native code-word lengths, where the row weights are typically high. For our simulations, we have considered a small 2-D page with multiple small LDPC codes interleaved, to ensure the computational feasibility of the GBP algorithm.

IV. Simulations and Results

We have simulated the TDMR channel using a Voronoi-based media model as proposed in [11]. The channel model parameters include grain size of CTC = 9 nm, bit-size = 18 nm × 18 nm, achieving a channel bit density of 1.8 Tb/in^2. The 2-D pages of size 128×256 data corresponding to 4 kB sector are generated at a time. The readback signal is generated using the Voronoi-based media model and is equalized using a 5×5 partial response (PR) equalizer for a 3×3 PR target designed under monic constraint as in [11].

A. Burst Erasure Correction Performance of the Proposed 2-D LDPC Code

We use the media defect model in [6] to introduce rectangular defects. The defect detector proposed in [6] is used at the output of 2-D Soft-output Viterbi algorithms to detect the location of the burst erasures and to indicate the LDPC decoder using the BP algorithm. The performance of the proposed 2-D LDPC code is compared against 1-D QC-LDPC code in the read channel architecture as in [6].

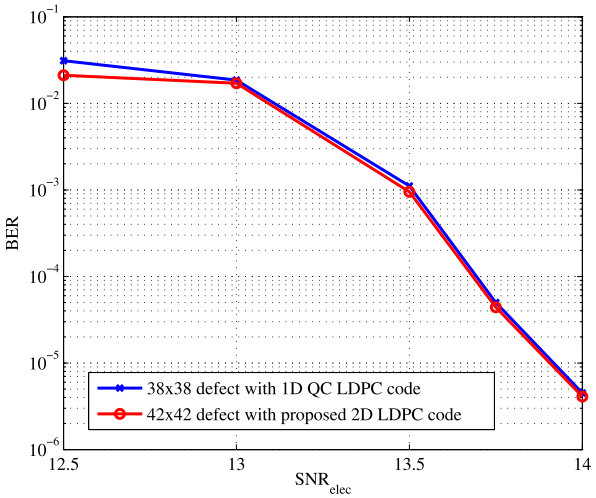

Fig. 6. BER performance of the proposed 2-D LDPC code is compared against a 1-D QC-LDPC code for burst erasure correction performance. The proposed 2-D LDPC code is able to correct bursts of >20% larger than the 1-D QC-LDPC code with a similar performance.

The 2-D LDPC code is constructed using a cube of size $p = 32$. For a 2-D code-word size of 128×256, we choose to construct parity check tensor $\mathbf{H}_{2\text{-D}}$ by filling $c \times h \times w = 128 \times 4 \times 8$. This gives us a code rate of $1-(128 \times 32/128 \times 256) = 0.875$, a row weight of 32, and a column weight of 4. The 1-D LDPC code of length $128 \times 256 = 32768$ b is designed

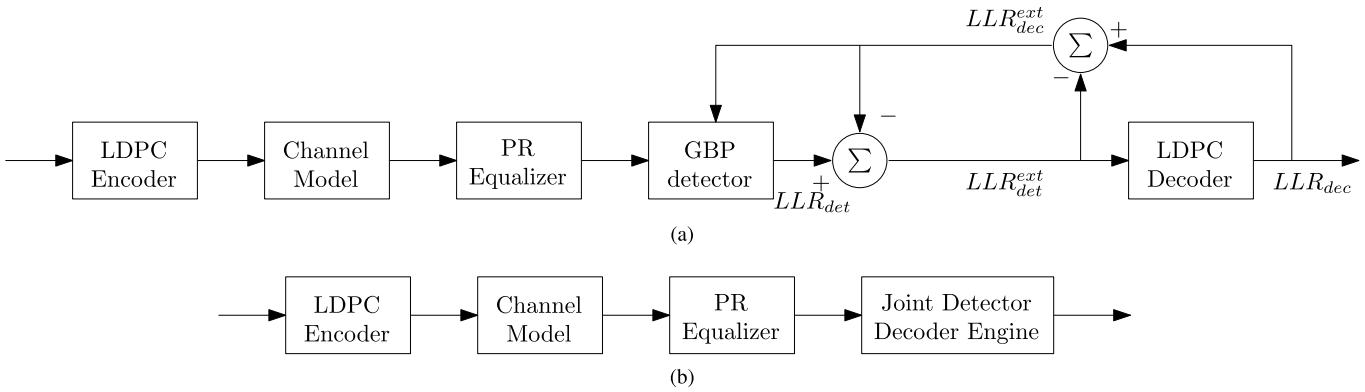

Fig. 7. Performance of joint detection and decoding engine is compared against the performance of an architecture with the detector operating in turbo loop with decoder. The same LDPC code and channel conditions are used. (a) Read channel architecture showing GBP-based ISI detector operating in a turbo loop with LDPC decoder. (b) Read channel architecture where the proposed joint detection and decoding engine is used.

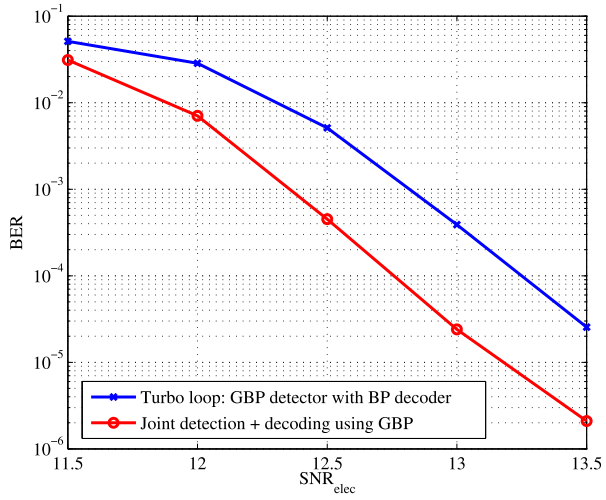

Fig. 8. BER performance proposed joint detection-decoder engine is compared against a traditional architecture, where the detector and the decoder operate in a turbo loop with six iterations. The proposed joint detection engine outperforms the turbo loop architecture by about 0.5 dB.

with a code rate of 0.87 and a circulant size of 1024. The 1-D codes are populated into the 2-D page in the raster order. The code rates are chosen such that the detector achieves a bit error rate (BER) of $\sim 1e-4$. This detector performance could achieve an SFR of $1e-15$ with a carefully designed LDPC codes.

Fig. 6 compares the performance of the TDMR channel using 1-D LDPC codes as against the proposed 2-D LDPC codes. We can see that the proposed 2-D LDPC codes are able to correct burst erasures of size 42×42 with the similar performance as 1-D LDPC codes with erasures of size 38×38. This is a significant (>20%) improvement in the burst erasure correction capability.

B. Performance of Joint Detection and Decoding Engine

To evaluate the performance of the joint detection and decoding engine proposed in Section III, we compare the performance of the following architectures.

1) A GBP-based detector followed by BP algorithm for LDPC decoding. The detector and the decoder operate in a turbo fashion [6] as shown in Fig. 7(a). The number of turbo iterations is limited to 6.
2) The PR equalized samples are jointly detected and decoded using the proposed algorithm in Section III as shown in Fig. 7(b).

Since the GBP algorithm is computationally not feasible for large page sizes, we have evaluated the performance on a small page size of 16×16. We expect higher gains using the joint detection and decoding engine for larger page sizes. Since the joint detection engine is limited by the row weight of the LDPC code, we have designed a 2-D LDPC code of size 8×16 with $p = 4$ and $c \times h \times w = 8 \times 2 \times 4$. The rows of two code words are alternatively interleaved to obtain a 2-D code word of size 16×16.

Fig. 8 compares the performance of the two architectures for a TDMR channel operating at 1.8 Tb/in^2 on pages of size 16×16. We observe that the proposed joint detection-decoder engine outperforms the turbo loop architecture by about 0.5 dB.

V. Conclusion

We have proposed the construction of a native 2-D LDPC code suitable for the correction of 2-D burst erasures. We have looked into the zero span of the codes and lower bounded the burst erasure size that the code can correct. The proposed code construction is observed to give a gain of >20% improvement in the burst erasure correction capability. We have also derived the GBP algorithm for joint detection and decoding by taking care of 2-D ISI constraints as well as the LDPC code constraints. The proposed joint detection and decoding engine is observed to give a gain of about 0.5 dB over an architecture, where separate detector and decoder operate in turbo fashion. It would be interesting to develop hardware architectures using field programmable gate array arrays and hardware acceleration engines toward performance assessment for large page sizes. The computational complexity of the GBP algorithm restricts its deployment for practical page sizes and large code lengths. Efficient hardware architectures of GBP need to be investigated.

Acknowledgment

This work was supported by the Indo-US Science and Technology Forum under Grant JC-Data Storage Research/16-2014.

REFERENCES

[1] R. Wood, M. Williams, A. Kavčić, and J. Miles, "The feasibility of magnetic recording at 10 terabits per square inch on conventional media," *IEEE Trans. Magn.*, vol. 45, no. 2, pp. 917–923, Feb. 2009.

[2] B. Vasić and M. E. Kurtas, *Coding and Signal Processing For Magnetic Recording Systems*. Boca Raton, FL, USA: CRC Press, 2004.

[3] M. P. C. Fossorier, "Quasicyclic low-density parity-check codes from circulant permutation matrices," *IEEE Trans. Inf. Theory*, vol. 50, no. 8, pp. 1788–1793, Aug. 2004.

[4] S. S. Garani and S. Parthasarathy, "Identifying a defect in a data-storage medium," U.S. Patent 9 324 370, Apr. 26, 2016.

[5] W. Tan, H. Xia, and J. R. Cruz, "Erasure detection algorithms for magnetic recording channels," *IEEE Trans. Magn.*, vol. 40, no. 4, pp. 3099–3101, Jul. 2004.

[6] C. K. Matcha and S. G. Srinivasa, "Defect detection and burst erasure correction for TDMR," *IEEE Trans. Magn.*, vol. 52, no. 11, Nov. 2016, Art. no. 3101211.

[7] S. Roy and S. G. Srinivasa, "Two dimensional error-correcting codes using finite field Fourier transform," in *Proc. IEEE Inf. Theory Workshop*, Oct. 2015, pp. 119–123.

[8] S. W. Yoon and J. Moon, "Two-dimensional error-pattern-correcting codes," *IEEE Trans. Commun.*, vol. 63, no. 8, pp. 2725–2740, Aug. 2015.

[9] M. Fossorier, "Universal burst error correction," in *Proc. IEEE Int. Symp. Inf. Theory*, Jul. 2006, pp. 1969–1973.

[10] Y. Chen and S. G. Srinivasa, "Joint self-iterating equalization and detection for two-dimensional intersymbol-interference channels," *IEEE Trans. Commun.*, vol. 61, no. 8, pp. 3219–3230, Aug. 2013.

[11] C. K. Matcha and S. G. Srinivasa, "Generalized partial response equalization and data-dependent noise predictive signal detection over media models for TDMR," *IEEE Trans. Magn.*, vol. 51, no. 10, Oct. 2015, Art. no. 3101215.

[12] S. Datta and S. G. Srinivasa, "Design architecture of a 2-D separable iterative soft-output Viterbi detector," *IEEE Trans. Magn.*, vol. 52, no. 5, May 2016, Art. no. 3500114.

[13] B. M. Kurkoski, P. H. Siegel, and J. K. Wolf, "Joint message-passing decoding of LDPC codes and partial-response channels," *IEEE Trans. Inf. Theory*, vol. 48, no. 6, pp. 1410–1422, Jun. 2002.

[14] W. Tan, S. Yang, K. Fitzpatrick, H. Zhong, L. Du, and Y. Lee, "Media defect recovery using full-response reequalization in magnetic recording channels," in *Proc. IEEE Globecomm*, Nov./Dec. 2008, pp. 1–5.

[15] G. Sridharan, A. Kumarasubramanian, A. Thangaraj, and S. Bhashyam, "Optimizing burst erasure correction of LDPC codes by interleaving," in *Proc. IEEE Int. Symp. Inf. Theory*, Jul. 2008, pp. 1143–1147.

[16] K. Li, A. Kavčić, and M. F. Erden, "Construction of burst-erasure efficient LDPC codes for use with belief propagation decoding," in *Proc. IEEE Int. Conf. Commun.*, May 2010, pp. 1–5.

[17] E. Paolini and M. Chiani, "Construction of near-optimum burst erasure correcting low-density parity-check codes," *IEEE Trans. Commun.*, vol. 57, no. 5, pp. 1320–1328, May 2009.

[18] Y. Cassuto and A. Shokrollahi, "LDPC codes for 2D arrays," *IEEE Trans. Inf. Theory*, vol. 60, no. 6, pp. 3279–3291, Jun. 2014.

[19] J. S. Yedidia, W. T. Freeman, and Y. Weiss, "Constructing free-energy approximations and generalized belief propagation algorithms," *IEEE Trans. Inf. Theory*, vol. 51, no. 7, pp. 2282–2312, Jul. 2005.

[20] C. K. Matcha, M. Bahrami, S. Roy, S. G. Srinivasa, and B. Vasić, "Generalized belief propagation based TDMR detector and decoder," in *Proc. IEEE Int. Symp. Inf. Theory*, Jul. 2016, pp. 210–214.

[21] S. M. Khatami and B. Vasić, "Generalized belief propagation detector for TDMR microcell model," *IEEE Trans. Magn.*, vol. 49, no. 7, pp. 3699–3702, Jul. 2013.

[22] P. Pakzad and V. Anantharam, "Estimation and marginalization using the Kikuchi approximation methods," *Neural Comput.*, vol. 17, pp. 1836–1873, Aug. 2003.